NASA TM X-115

TECHNICAL MEMORANDUM

X-115

AERODYNAMIC CHARACTERISTICS AT MACH NUMBER 2.01 OF AN AIRPLANE CONFIGURATION HAVING A CAMBERED AND TWISTED ARROW WING DESIGNED FOR A MACH NUMBER OF 3.0

By Odell A. Morris and A. Warner Robins

Langley Research Center
Langley Field, Va.

Declassified September 1, 1961

NATIONAL AERONAUTICS AND SPACE ADMINISTRATION

WASHINGTON September 1959

NATIONAL AERONAUTICS AND SPACE ADMINISTRATION

TECHNICAL MEMORANDUM X-115

AERODYNAMIC CHARACTERISTICS AT MACH NUMBER 2.01 OF AN AIRPLANE CONFIGURATION HAVING A CAMBERED AND TWISTED ARROW WING DESIGNED FOR A MACH NUMBER OF 3.0*

By Odell A. Morris and A. Warner Robins

SUMMARY

An investigation has been conducted to determine the aerodynamic characteristics in pitch at Mach number 2.01 of an airplane configuration having an arrow wing with 75° of leading-edge sweep and with camber and twist to produce an optimum load distribution at a lift coefficient of 0.1 and a Mach number of 3.0. NACA RM L58E21 reports the results of previous tests of the same airplane configuration at Mach numbers of 2.36 and 2.87. The aspect ratio for the configuration is 1.79, and wing-thickness ratios normal to the leading edges vary from 8 to 14 percent. Tests of the complete configuration and of various combinations of components were made with the original wing apex and the modified wing apex. Additional tests were made to determine the effects of wing fences and wing-body-juncture fairings on the upper-surface flow.

Reynolds number for all tests, based on the mean geometric chord, was 5.8×10^6. Transition was fixed near the leading edges of all components.

The maximum lift-drag ratio of 7.0 for the complete configuration at Mach number 2.01 showed little or no increase over that previously measured at Mach number 2.36. Luminescent-oil-flow studies showed that despite the lower initial component of velocity normal to the leading edges at Mach number 2.01, the flow separated in the same manner as it had at Mach numbers of 2.36 and 2.87. The use of fences and large wing-body-juncture fairings increased the lift-drag ratio by about 0.3. The lift-drag ratio was essentially unaffected by the appreciable modification of the wing apex.

INTRODUCTION

Reference 1 describes in detail an experimental investigation in the Langley Unitary Plan wind tunnel at Mach numbers of 2.36 and 2.87 of an airplane configuration having a highly swept arrow wing cambered and twisted to provide an optimum load distribution at a lift coefficient of 0.1 and a Mach number of 3.0. Reference 2 briefly summarizes the results for the same configuration at a Mach number of 2.87 and compares these results with those for several configurations designed to satisfy the same requirements. The lift-drag ratios reported in reference 1 for the tests at Mach numbers 2.36 and 2.87 were considerably below those anticipated. In the analysis of these data, reference 1 indicates that the performance deficiency appeared to be the result of extensive upper-surface flow separation arising from cross-flow Mach numbers greater than unity. An increase in lift-drag ratio was noted when Mach number was decreased from 2.87 to 2.36. Because the cross-flow component at low lift coefficients might be subcritical at a Mach number of 2.01 and might produce clean upper-surface flow, the present brief investigation was initiated at the Langley 4- by 4-foot supersonic pressure tunnel.

For the tests of this configuration at a Mach number of 2.01, the Reynolds number based on the mean geometric chord was 5.8×10^6, and transition was fixed near the leading edges of all components. The angle of attack was varied from -4° to 8°. Tests were made of the complete configuration and of the various combinations of components. In order to improve upper-surface flow, some tests were made with wing fences, with generous fairings at the wing-body junctures, or with both fences and fairings. The results are presented with limited analysis.

SYMBOLS

C_D drag coefficient, $\frac{\text{Drag}}{qS}$

C_L lift coefficient, $\frac{\text{Lift}}{qS}$

C_m pitching-moment coefficient (reference center located at apex of wing trailing edge), $\frac{\text{Pitching moment}}{qS\bar{c}}$

$\bar{c}$ wing mean aerodynamic chord, in.

L/D lift-drag ratio

q	free-stream dynamic pressure, lb/sq ft
S	total wing area, sq ft
α	angle of attack of balance axis (balance axis is 2° noseup relative to wing reference plane), deg
β	Mach number parameter, $\sqrt{M^2 - 1}$

Subscript:

max	maximum

Components:

B	body
B'	body with large body-wing fairing
F	vertical fins
N	nacelles and pylons
W	wing
W'	wing with modified wing-apex section
W_f	wing with fences

MODELS AND EQUIPMENT

The principal dimensions of the complete model and of the wing-body configurations are presented in the three-view drawings of figure 1. The 75° swept arrow-wing model, which was designed to meet the volume requirements of a Mach number 3 long-range bomber, was first tested in the Langley Unitary Plan wind tunnel. Reference 1 reports the results of these tests, describes the model design in detail, and shows dimensions of all the model components.

The wing and fuselage were constructed of aluminum and were sting-mounted with a six-component strain-gage balance enclosed within the fuselage. Pressure orifices were provided inside the fuselage base for the measurement of base pressure. Total and static pressures were measured at the exits of two nacelles (one inboard and one outboard) by means of sting-mounted rakes. The exit diameters of the nacelles were

enlarged 0.050 inch, and boundary-layer transition was fixed on the inlet spikes in order that the inlets be started. In an attempt to improve the flow over the upper surface of the wing, the original model was also tested with fairings added at the wing-body juncture and with a fence mounted on each semispan. The fairings were tangent to the wing surfaces and completely covered the discontinuity in the upper-surface wing juncture and the portion of the fuselage ahead of the cylindrical section. From the forward part of the cylindrical fuselage section toward the rear, the fairings were tangent to both the fuselage and wing surfaces and diminished in radii until they disappeared at a station approximately 28 inches from the wing apex. (See fig. 1(b).) The fences were constructed of $\frac{1}{16}$-inch-thick steel and were fitted to the wing normal to the local wing surface. The leading edges of the fences were swept approximately 45° with respect to the local wing surface and were sharpened to a 10° wedge. The height above the local surface of the wing varied linearly from 1/2 inch at the front of the fence to 3/4 inch at the wing trailing edge. Fence locations are shown in figure 1(b).

Tests were also made with a modified wing-apex section on the original model. Approximately 9 inches of the original wing apex was cut off and was replaced with a modified wing-apex section. (See fig. 1(c).) The modified wing-apex section differed from the original in that its cross sections normal to the model axis formed essentially flat outlines instead of the inverted vee cross sections formed by the original wing-apex section. Also, the wing apex was lower for the modified section than for the original section. Ordinates for the modified wing-apex section are given in table I.

TESTS

The tests were conducted in the Langley 4- by 4-foot supersonic pressure tunnel at a Mach number of 2.01, a stagnation pressure of 14.5 lb/sq in., and a stagnation temperature of 110° F. The Reynolds number based on $\bar{c}$ was 5.8×10^6. The stagnation dewpoint was low enough (-25° F or less) to avoid significant condensation effects. The models were sting-mounted, and pitch tests of the complete models were made for an angle-of-attack range of about -4° to 10°.

All tests were made with fixed transition. The transition strips were 1/8-inch-wide bands of No. 60 carborundum grains sparsely applied to the surfaces with plastic spray. The bands were located on both surfaces of the wing, on the fins, and around each of the six nacelles approximately 1/4 inch from the leading edges of the various components in a streamwise direction.

A flow-visualization technique, which utilized a fluorescent oil painted on the wing surface, was also employed for some tests. The photographs of the wing surface, made with the tunnel in operation, indicate airflow direction on the surface.

CORRECTIONS AND ACCURACY

The angles of attack have been corrected for deflection of the sting and balance under load. The force data have been corrected to make the base pressures correspond to the free-stream static pressure. The axial-force data were corrected to remove the contribution of internal drag of the six nacelles.

An estimate of the probable errors introduced in the present data and based upon the balance accuracy and the repeatability of the data is as follows:

C_L	±0.002
C_D	±0.0004
C_m	±0.002
α, deg	±0.10

PRESENTATION OF RESULTS

The results of this investigation are presented in the following figures:

	Figure
Aerodynamic characteristics of the original wing-body configuration alone, with fins, and with fins and nacelles	2
Aerodynamic characteristics of the modified wing-body configuration alone, with fins, and with fins and nacelles	3
Comparison of the aerodynamic characteristics of the original wing-body configuration with the modified wing-body configuration	4
Comparison of the aerodynamic characteristics of the complete configuration with the original wing apex with complete configuration with the modified wing apex	5

RESULTS AND DISCUSSION

Wing-Body Configuration

Maximum lift-drag ratio for the wing-body configuration was approximately 8.0. The experimental value of $\frac{C_D}{\beta C_L^2}$ at Mach number 2.01 was approximately 0.29, which is much higher than the theoretical value of about 0.15 for a wing of this plan form designed in a similar manner for Mach number 2.0. The theoretical value of $\frac{C_D}{\beta C_L^2}$ for the design Mach number of 3.0 was coincidentally 0.15, also. (See fig. 3 of ref. 3.) The experimental value of $\frac{C_D}{\beta C_L^2}$ in reference 1 for Mach number 2.87 was about 0.27. Although the wing shape, which may have been far from optimum at Mach number 2.01, could be partially responsible for the high drag due to lift, the oil-flow photographs of the wing-body configurations (figs. 7(a) and 8(a)) indicate that the fault is largely due to areas of separated flow extending all the way out to the wing tips. The early separation of the flow at the wing tips is reflected in the "pitch-up" property of the pitching-moment curves (fig. 4(a)).

Effect of Vertical Fins

The addition of vertical fins to the wing-body configuration with either the original or modified wing apex increased the lift-curve slope (figs. 2(a) and 3(a)). This increase together with a reduction in the drag increment due to the addition of fins as angle of attack increased, provided a lower drag due to lift (fig. 11) than was obtained with the

wing-body configuration without fins. Comparison of the oil-flow photographs of the configuration with fins with those of the configuration without fins (figs. 7 and 8) shows that the addition of fins reduced the extent of flow separation by preventing the separation in the inboard regions from spreading to the wing tips. The "fencing" effects of the fins is probably most apparent in the comparison of the pitching-moment data for the configurations with and without fins (figs. 2(a) and 3(a)). The addition of fins and the attendant retention of lift at the wing tips are seen to produce a much more linear pitching-moment curve.

Effects of Wing-Apex Shape

Comparison of the data for the wing-body configuration with the original wing apex with the configuration with modified wing apex shows little if any change in lift-curve slope or drag below maximum lift-drag ratio (fig. 4). The drag due to lift appears to be slightly lower at the higher lift coefficients for the configuration with the original wing apex (fig. 11). Oil-flow photographs (fig. 8) show that the modified wing apex generated two strong vortices at the nose of the configurations. The complete configuration with the modified wing apex showed a higher trim lift coefficient and somewhat less stability (fig. 5) than the complete configuration with the original wing apex. Some improvement might have resulted if the modified apex had been positioned at a lower angle to effect a reduction in vorticity over the wing-apex section and a smoother upwash distribution ahead of the remainder of the span.

Effect of Engine Nacelles

Engine nacelles provided an interference lift as evidenced by the lift curves of figures 2 and 3. The change in longitudinal trim (figs. 2 and 3) must arise from the interference field of the nacelles which were located on the rearward portions of the wing. It should be noted here that the inlets, which were designed for Mach number 3.0, were operating in an off-design condition (center-body shock well ahead of the inlet lips). Less interference effects would be expected for inlets designed for the test Mach number. The drag increment due to the addition of the six nacelles was about 0.0018 at zero lift (figs. 2(a) and 3(a)).

Effects of Fairings and Fences

The oil-flow photographs (fig. 9) show cleaner flow near the wing-body juncture when fairings were used. Figure 10 indicates that the addition of fences reduces the extent of upper-surface flow separation.

This reduction resulted in an increase in lift-curve slope (fig. 6). The lift-drag ratio for the complete configuration with fairings and fences was increased to approximately 7.3.

Summary of Lift-Drag Ratio Results

Maximum lift-drag ratio of the wing-body configuration with either the original wing apex or the modified wing apex was approximately 8.0 (figs. 2(a) and 3(a)). The addition of fins reduced the maximum lift-drag ratio to about 7.6. Addition of nacelles (constituting a complete configuration without fairings or fences) resulted in a maximum lift-drag ratio of approximately 7.0 (figs. 2(a) and 3(a)). The further addition of fairings and fences raised the maximum lift-drag ratio to about 7.3 (fig. 6(a)).

Figure 12 compares the present results with those of reference 1. The improvement in upper-surface flow and the attendant increase in lift-drag ratio expected with the reduction of the component of velocity normal to the leading edge when Mach number was reduced from 2.36 to 2.01 did not materialize. The favorable effect of reducing the initial velocity component normal to the leading edge (ref. 3) appears to have been offset by an increase in lift requirement and in induced velocity normal to the leading edge.

CONCLUDING REMARKS

An investigation has been conducted to determine the aerodynamic characteristics in pitch at Mach number 2.01 of an airplane configuration having an arrow wing with 75° of leading-edge sweep and with camber and twist to produce an optimum load distribution at a lift coefficient of 0.1 and a Mach number of 3.0. Reynolds number for all tests, based on the mean geometric chord, was 5.8×10^{6}. Transition was fixed near the leading edges of all components.

The maximum lift-drag ratio of 7.0 for the complete configuration at Mach number of 2.01 showed little or no increase over that previously measured at Mach number 2.36. Luminescent-oil-flow studies showed that despite the lower initial component of velocity normal to the leading edges at Mach number 2.01, the flow separated in the same manner as it had at Mach numbers of 2.36 and 2.87. The use of fences and large wing-body-juncture fairings increased the lift-drag ratio by about 0.3. The

lift-drag ratio was essentially unaffected by the appreciable modification of the wing apex.

Langley Research Center,
National Aeronautics and Space Administration,
Langley Field, Va., May 27, 1959.

REFERENCES

1. Hallissy, Joseph M., Jr., and Hasson, Dennis F.: Aerodynamic Characteristics at Mach Numbers 2.36 and 2.87 of an Airplane Configuration Having a Cambered Arrow Wing With a 75° Swept Leading Edge. NACA RM L58E21, 1958.

2. Baals, Donald D., Toll, Thomas A., and Morris, Owen G.: Airplane Configurations for Cruise at a Mach Number of 3. NACA RM L58E14a, 1958.

3. Brown, Clinton E., and McLean, Francis E.: The Problem of Obtaining High Lift-Drag Ratios at Supersonic Speeds. Preprint No. 844, S.M.F. Pub. Fund Preprint, Inst. Aero. Sci., Inc., July 1958.

TABLE I.- WING ORDINATES FOR MODIFIED WING-APEX SECTION

[All dimensions are in inches. Ordinates to the upper and lower surfaces, z_u and z_l, are measured normal to wing reference plane which is parallel to free stream when the wing is at design attitude. Ordinates are positive upward.]

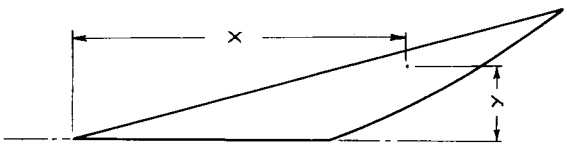

y	z_u	z_l
x = 0		
0.000	2.200	2.200
x = 1.553		
0.000	2.058	1.682
.075	2.023	1.692
.150	1.985	1.700
.225	1.950	1.712
.300	1.906	1.727
.375	1.852	1.746
.416	1.805	1.805
x = 3.106		
0.000	1.832	1.247
.075	1.813	1.262
.150	1.798	1.277
.225	1.776	1.287
.300	1.756	1.297
.375	1.732	1.305
.450	1.705	1.312
.525	1.671	1.317
.600	1.632	1.320
.675	1.586	1.331
.750	1.526	1.347
.800	1.473	1.373
.8323	1.418	1.418
x = 4.659		
0.000	1.561	0.846
.075	1.574	.875
.150	1.583	.899
.225	1.583	.919
.300	1.574	.937
.375	1.562	.948
.450	1.550	.958
.525	1.530	.968
.600	1.507	.975
.675	1.480	.985
.750	1.449	.992
.825	1.417	.998
.900	1.375	1.003
.975	1.330	1.004
1.050	1.279	1.006
1.125	1.218	1.010
1.200	1.137	1.015
1.2484	1.047	1.047

y	z_u	z_l
x = 6.212		
0.000	1.282	0.457
.075	1.312	.497
.150	1.337	.538
.225	1.362	.572
.300	1.359	.597
.375	1.360	.616
.450	1.357	.630
.525	1.351	.643
.600	1.341	.653
.675	1.327	.662
.750	1.307	.669
.900	1.258	.677
1.050	1.202	.679
1.200	1.136	.678
1.350	1.043	.674
1.500	.918	.668
1.625	.788	.666
1.6645	.705	.705
x = 7.765		
0.000	0.993	0.093
.075	1.037	.143
.150	1.077	.190
.225	1.106	.236
.300	1.128	.271
.375	1.142	.300
.450	1.149	.321
.600	1.148	.352
.750	1.130	.371
.900	1.098	.377
1.050	1.062	.3785
1.200	1.009	.378
1.350	.950	.372
1.500	.879	.363
1.650	.803	.357
1.800	.719	.356
1.950	.610	.360
2.0806	.405	.405
x = 9.318		
0.000	0.698	-0.255
.075	.751	-.193
.150	.802	-.134
.255	.843	-.083
.300	.877	-.042
.375	.905	-.007
.450	.923	.023
.600	.940	.063
.750	.939	.086
.900	.926	.098
1.050	.906	.106
1.200	.873	.112
1.350	.837	.118
1.500	.797	.123
1.650	.753	.128
1.800	.707	.133
1.950	.652	.140
2.100	.582	.146
2.250	.491	.152
2.400	.378	.174
2.497	.228	.228

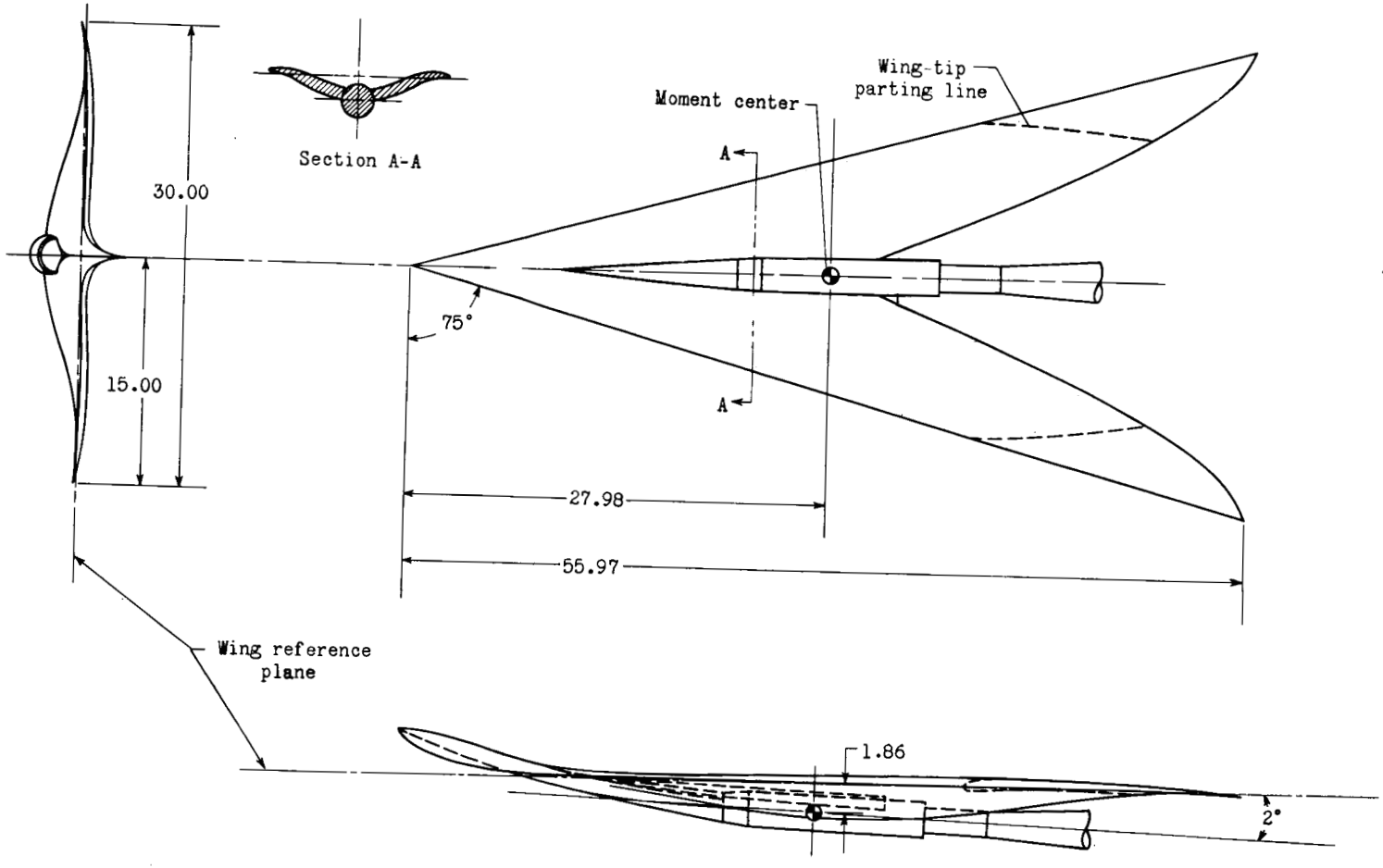

(a) Wing-body configuration with original wing-apex section.

Figure 1.- Three-view drawings of test configurations. All linear dimensions are in inches.

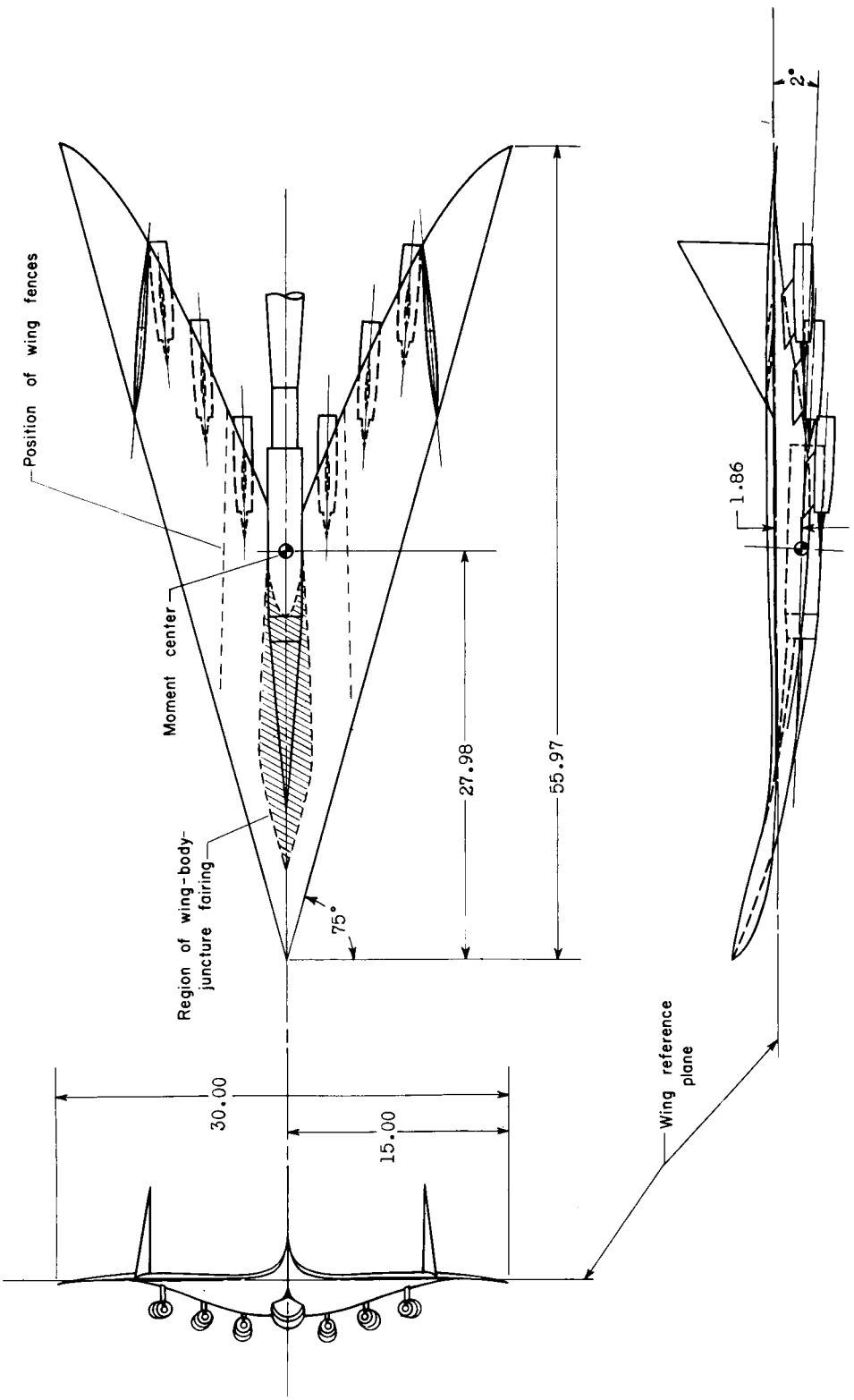

(b) Complete model configuration with fins and six nacelles.

Figure 1.- Continued.

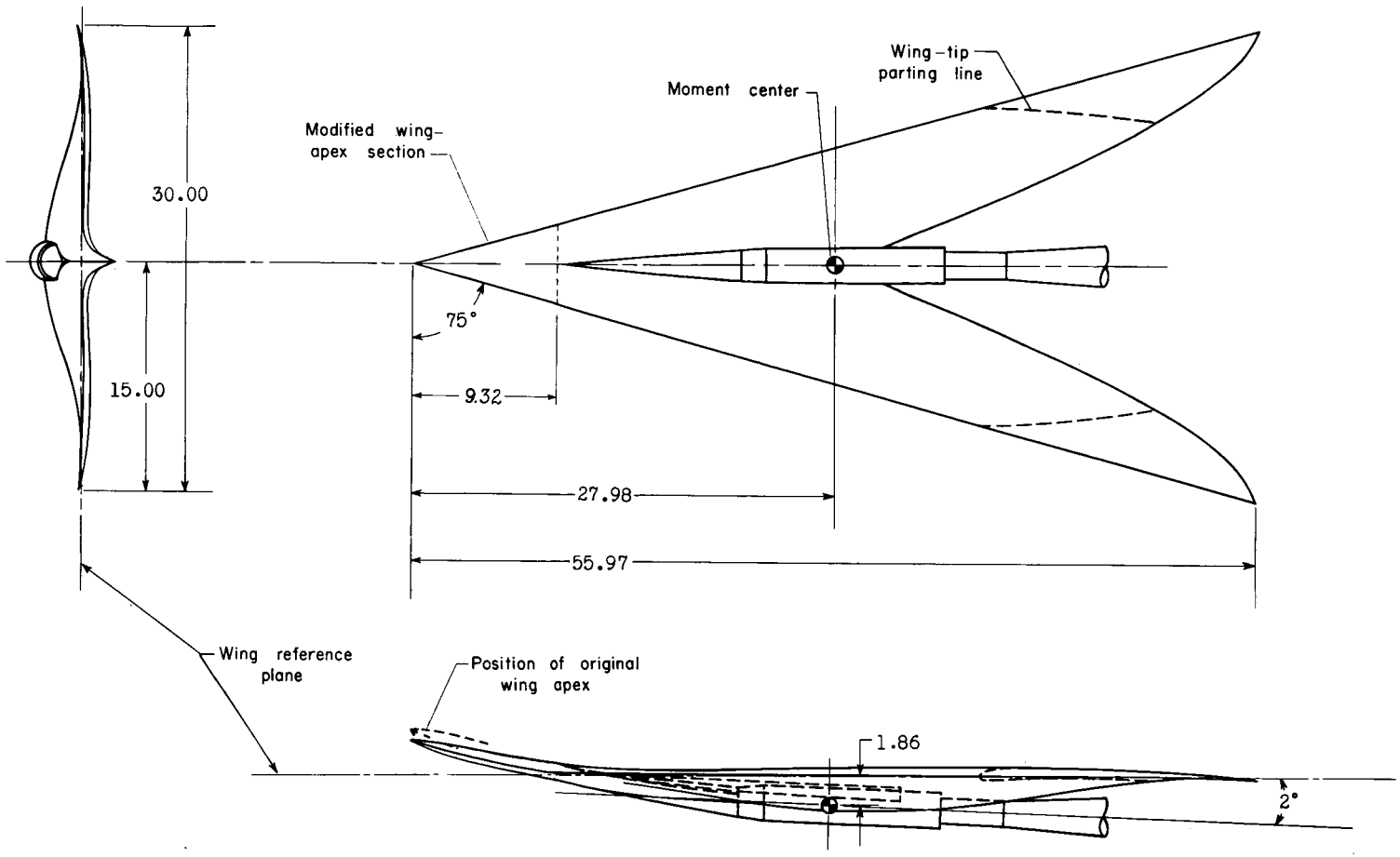

(c) Wing-body configuration with modified wing-apex section.

Figure 1.- Concluded.

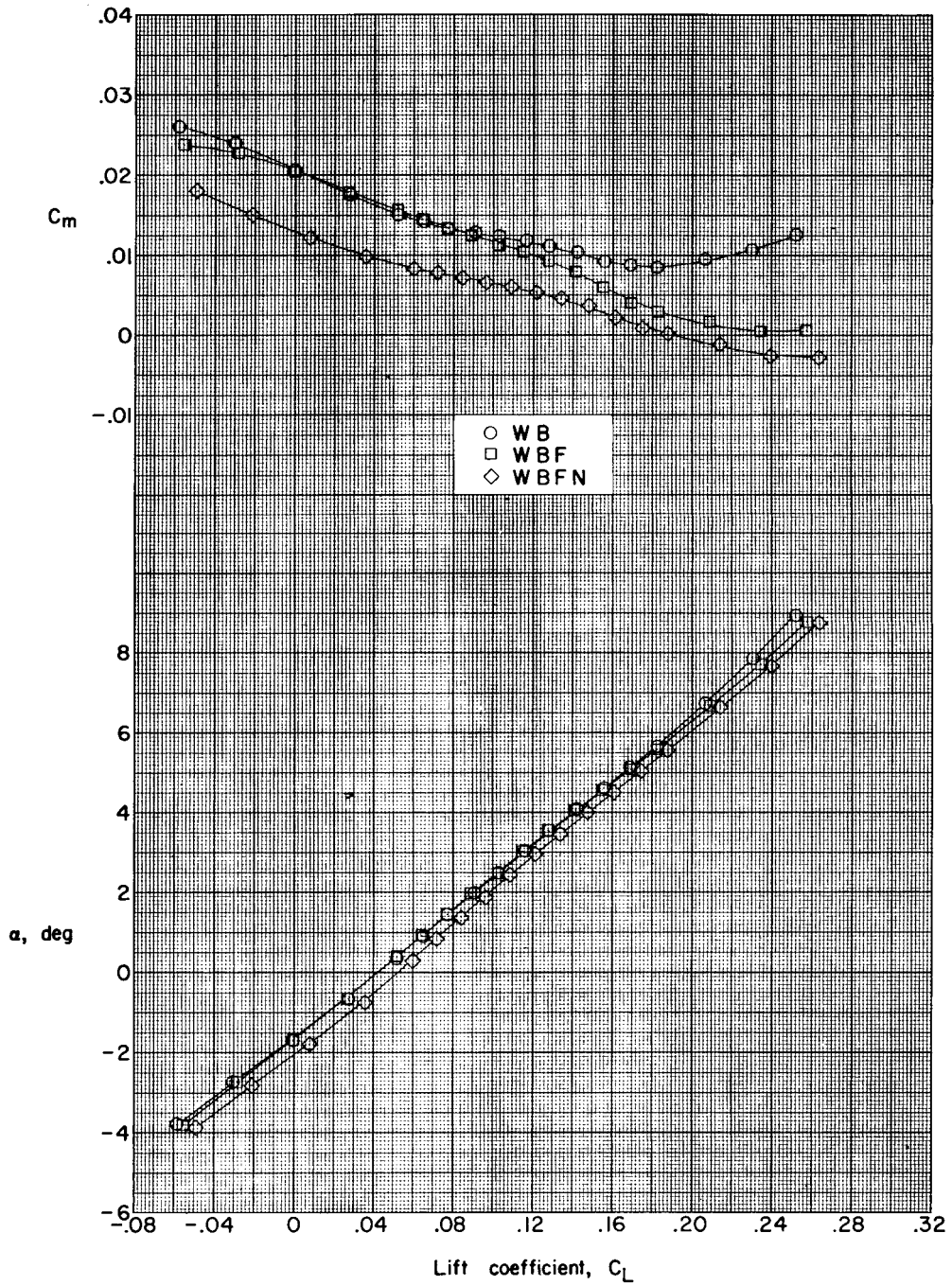

(a) Variation of C_m and α with C_L.

Figure 2.- Aerodynamic characteristics of the original wing-body configuration alone, with fins, and with fins and nacelles.

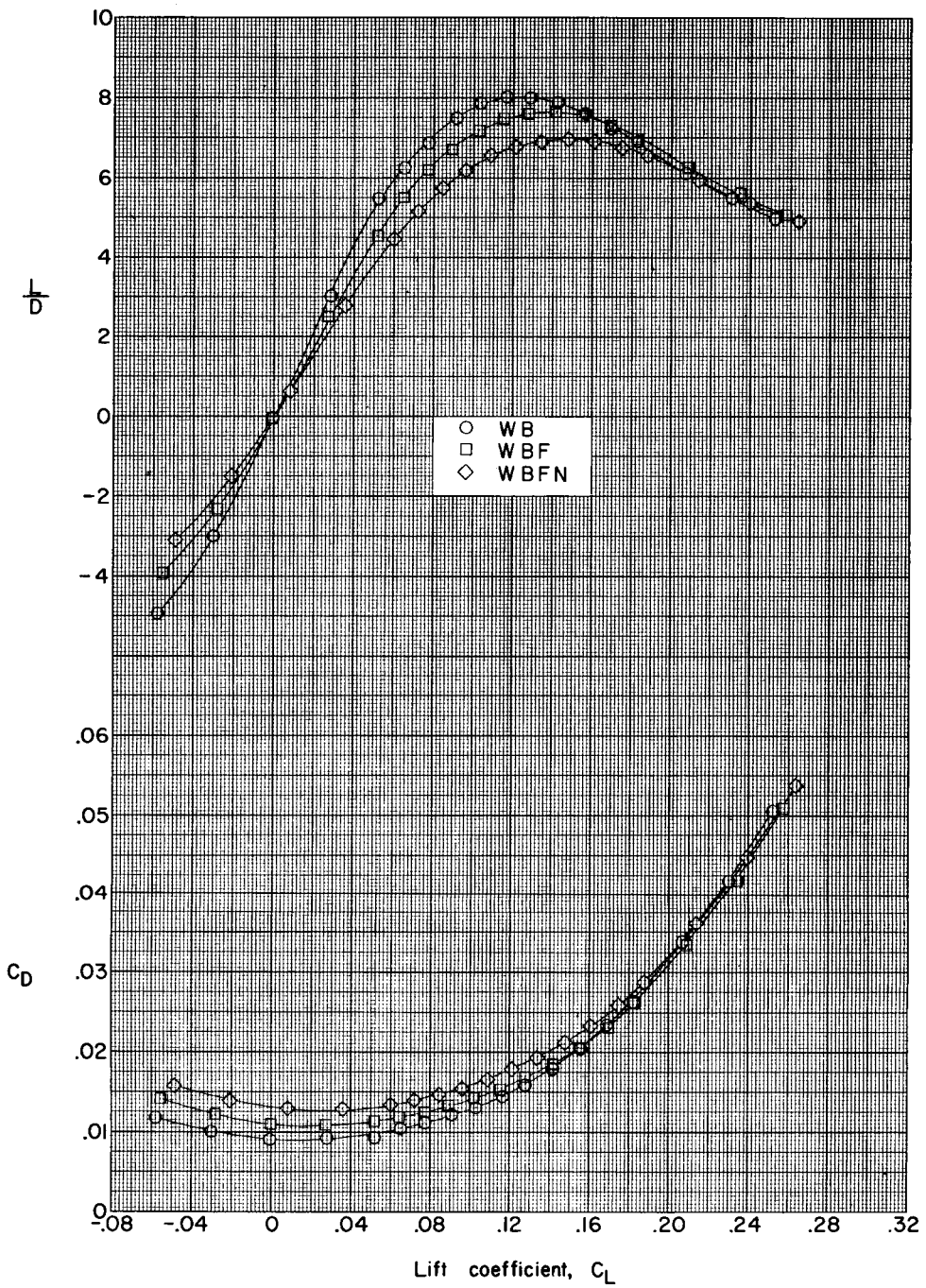

(b) Variation of L/D and C_D with C_L.

Figure 2.- Concluded.

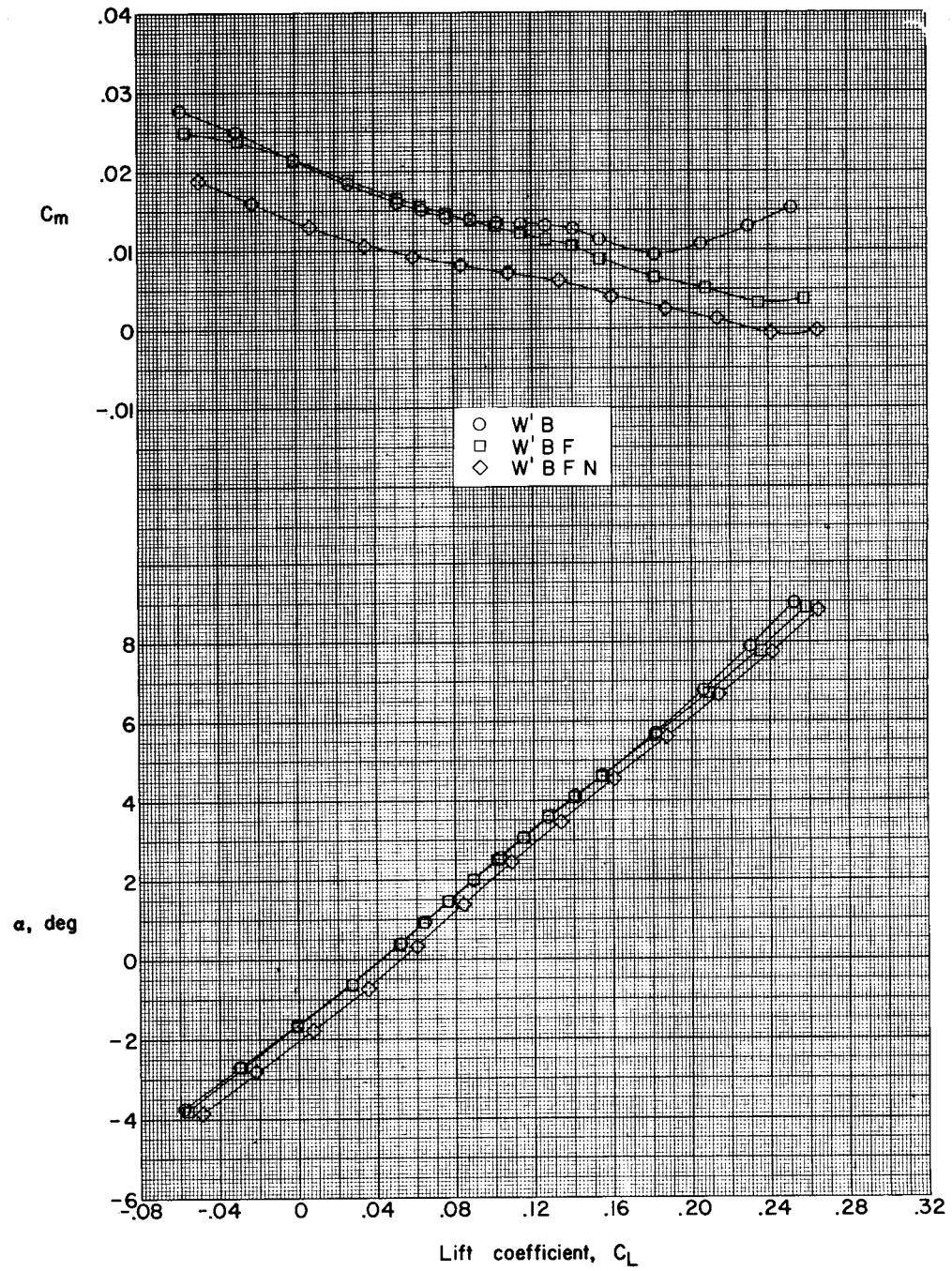

(a) Variation of C_m and α with C_L.

Figure 3.- Aerodynamic characteristics of the modified wing-body configuration alone, with fins, and with fins and nacelles.

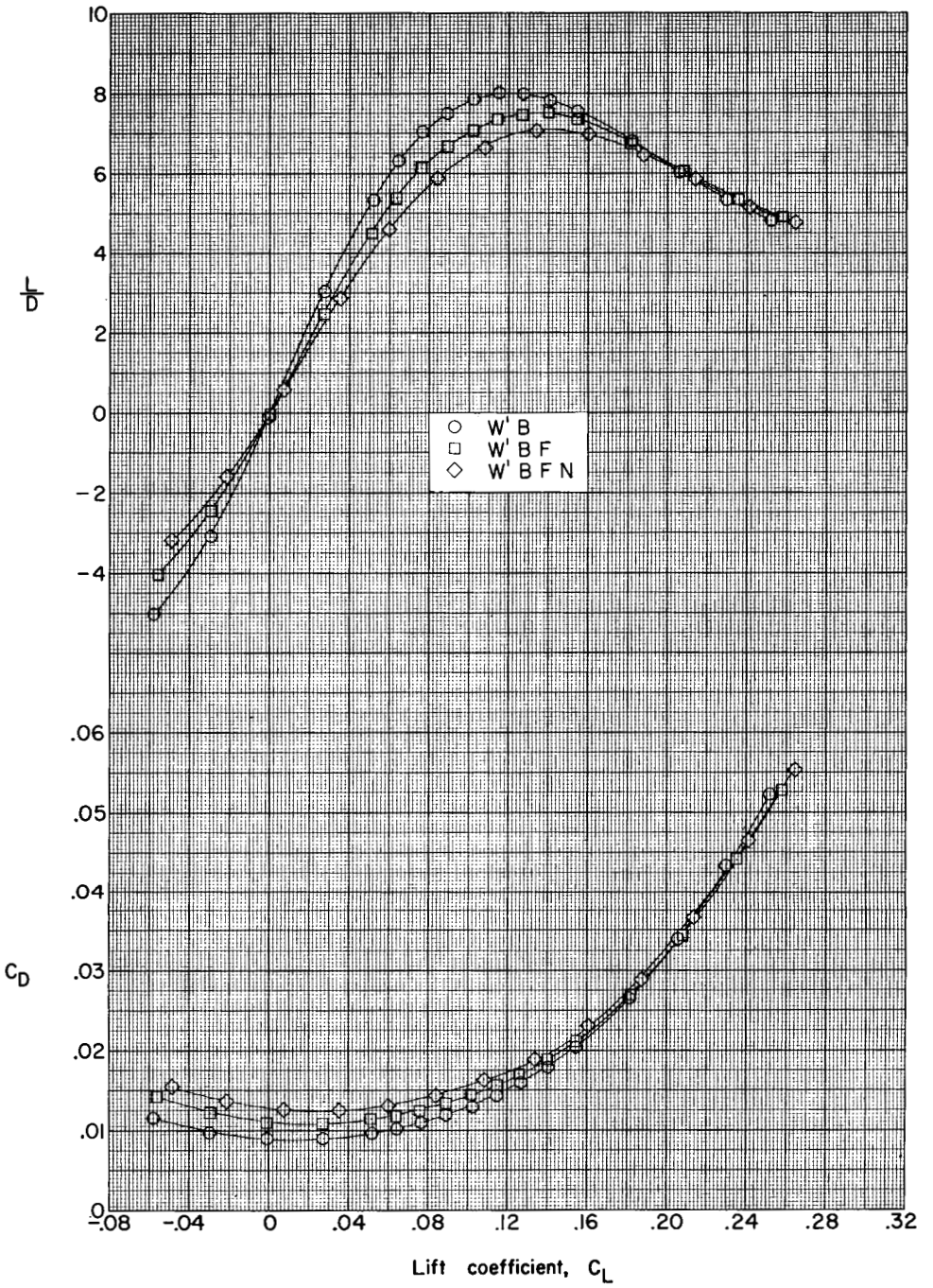

(b) Variation of L/D and C_D with C_L.

Figure 3.- Concluded.

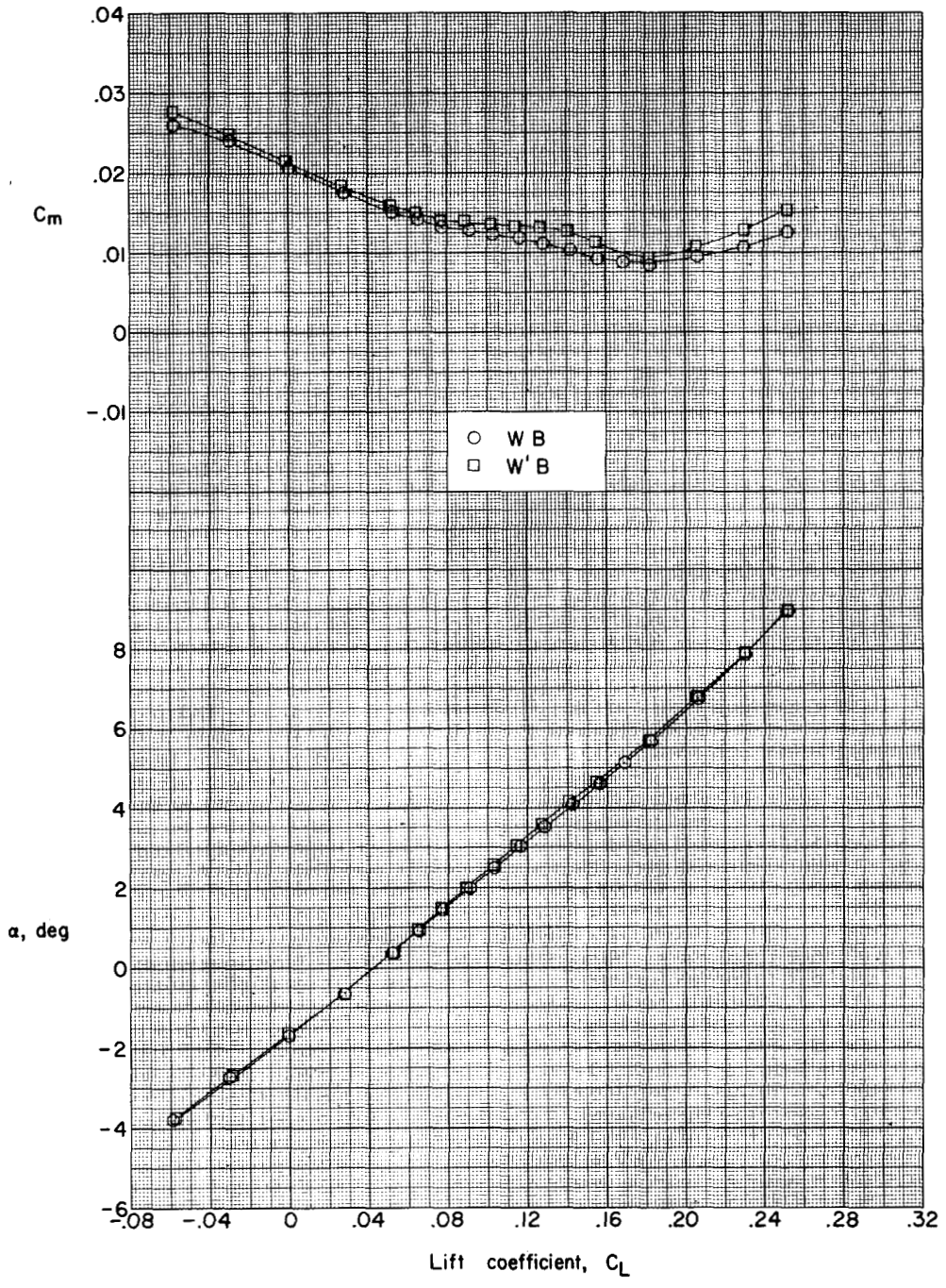

(a) Variation of C_m and α with C_L.

Figure 4.- Comparison of the aerodynamic characteristics of the original wing-body configuration with those of the modified wing-body configuration.

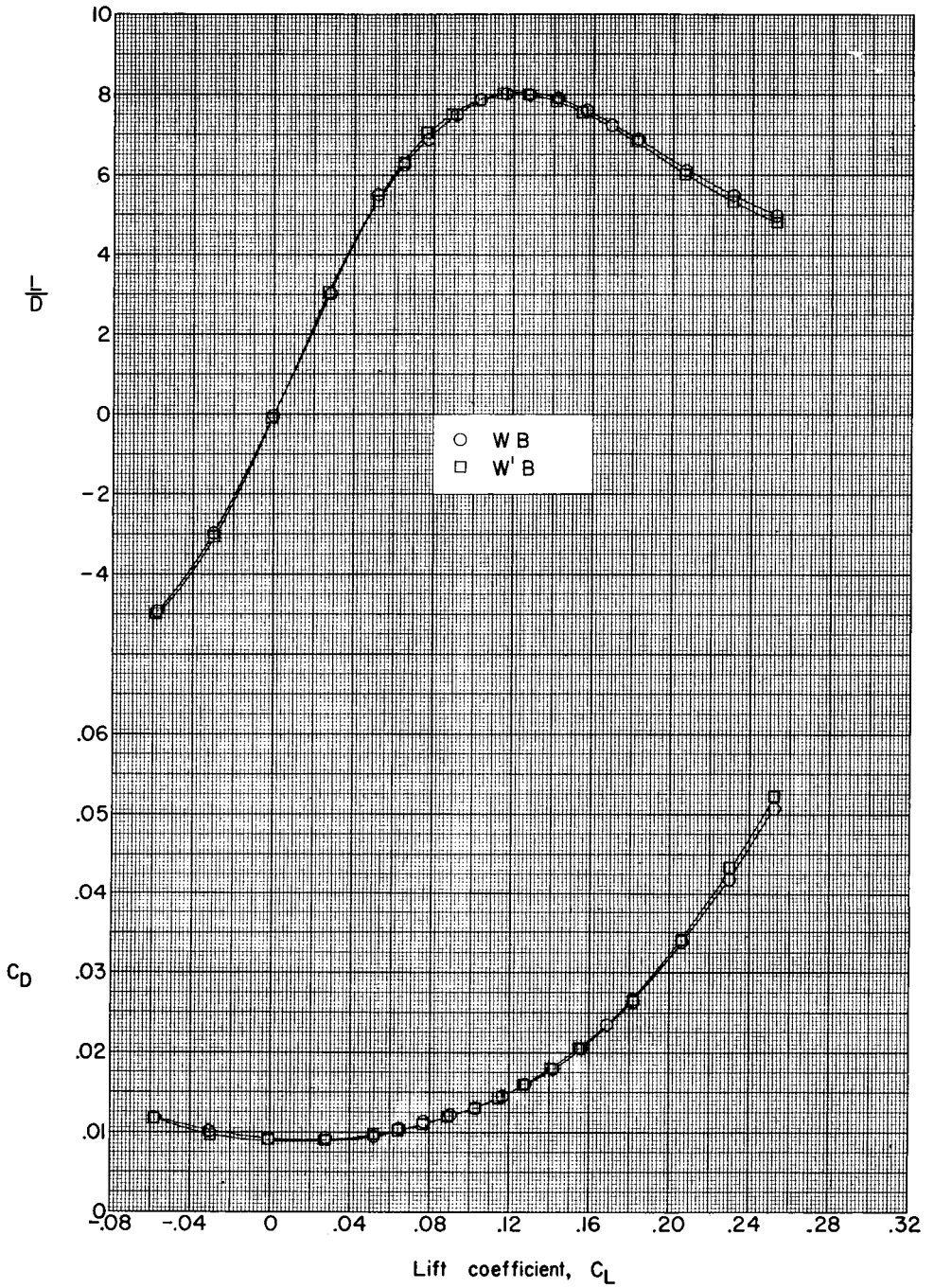

(b) Variation of L/D and C_D with C_L.

Figure 4.- Concluded.

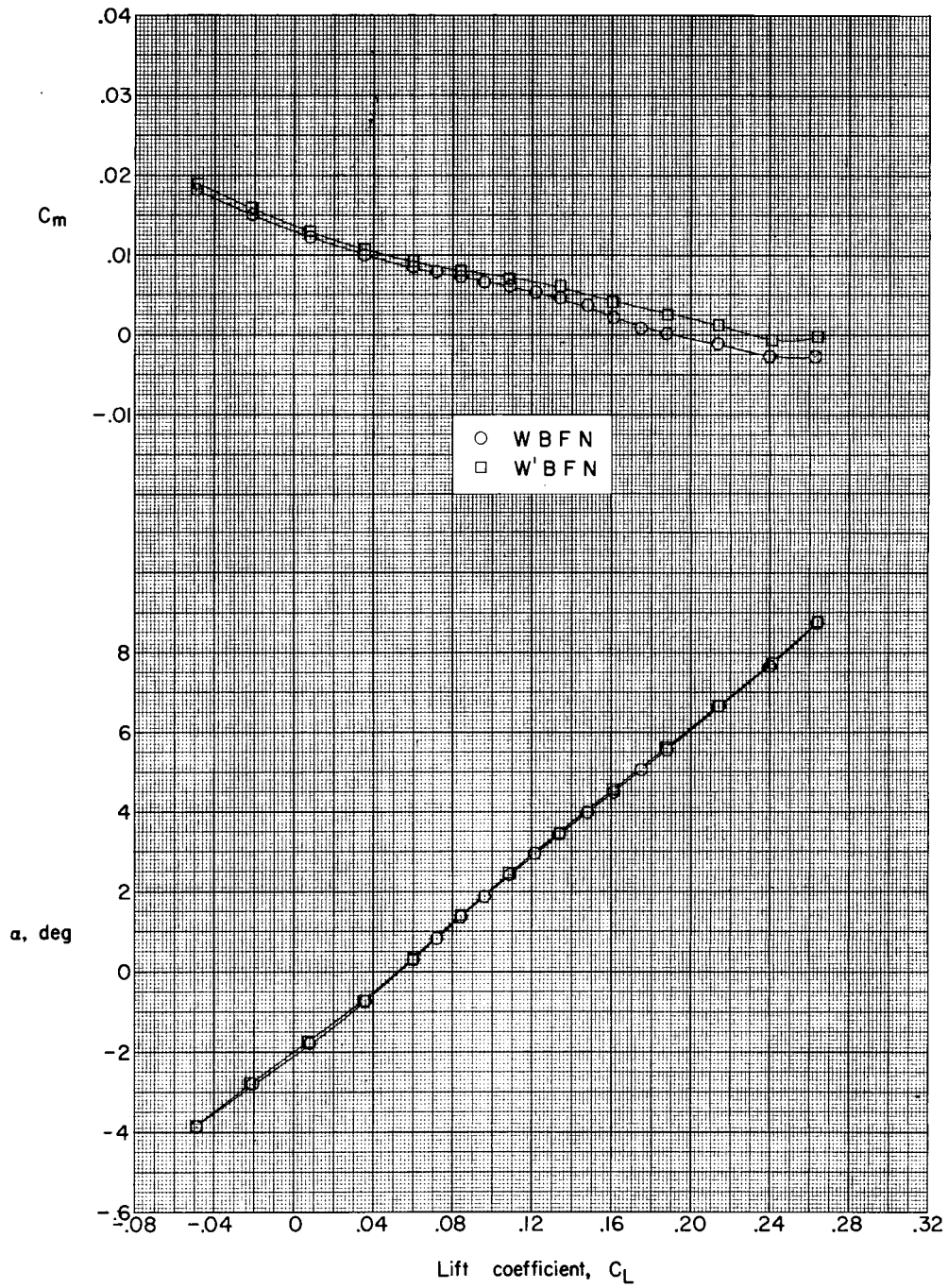

(a) Variation of C_m and α with C_L.

Figure 5.- Comparison of the aerodynamic characteristics of the complete configuration with the original wing apex with the complete configuration with the modified wing apex.

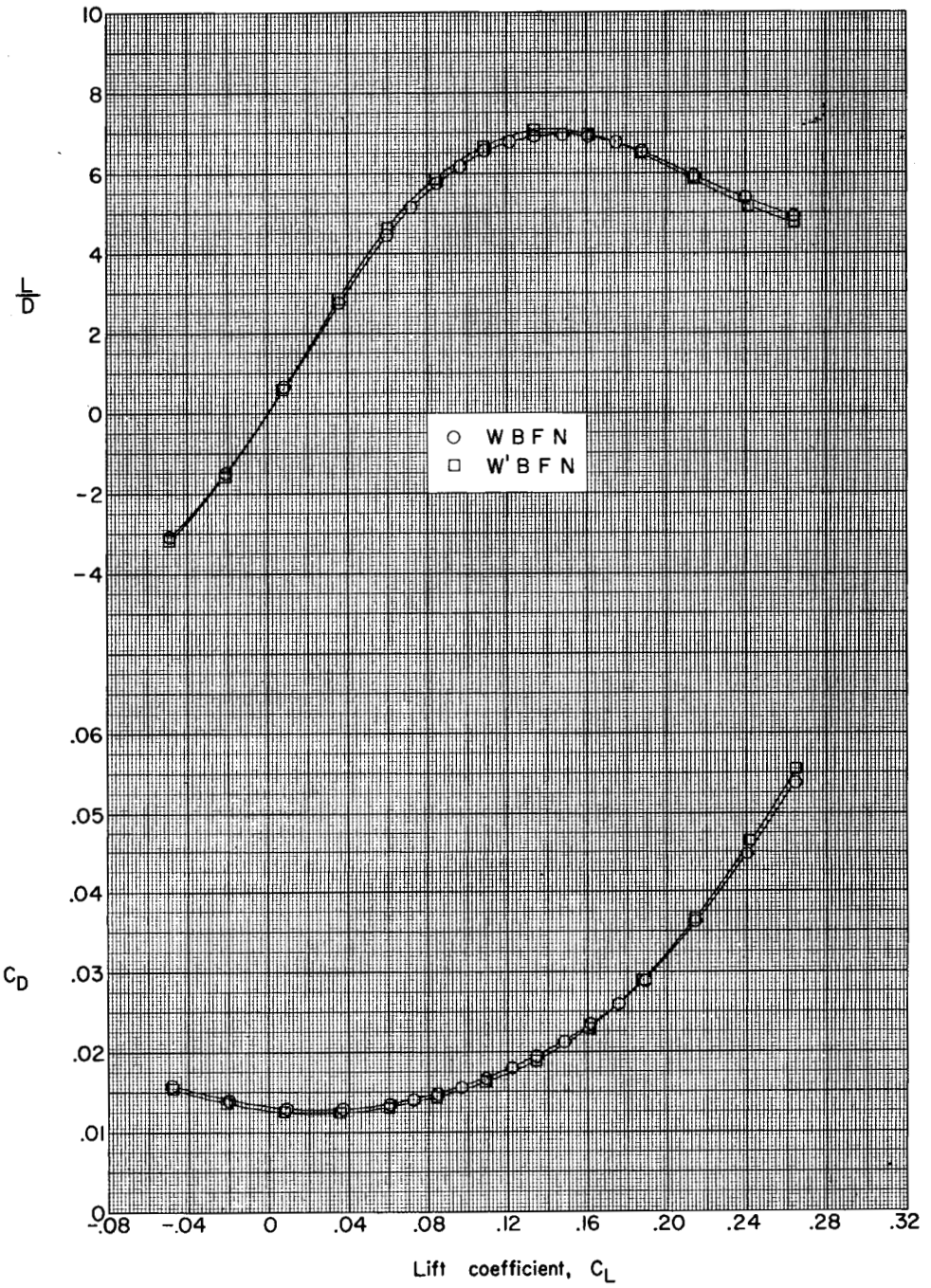

(b) Variation of L/D and C_D with C_L.

Figure 5.- Concluded.

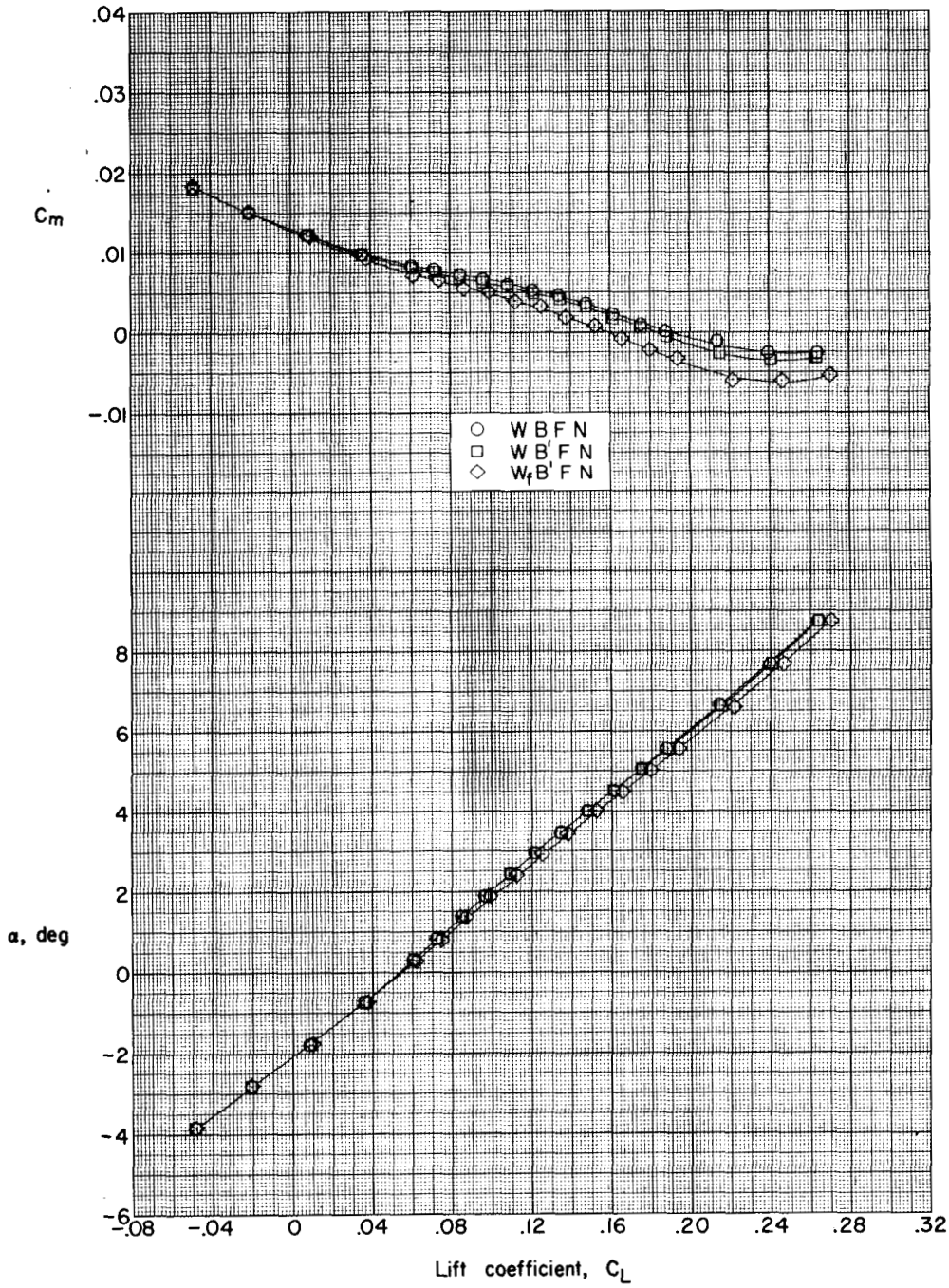

(a) Variation of C_m and α with C_L.

Figure 6.- Aerodynamic characteristics of the complete configuration (original wing apex) alone, with wing-body fairing, and with wing-body fairing and wing fences.

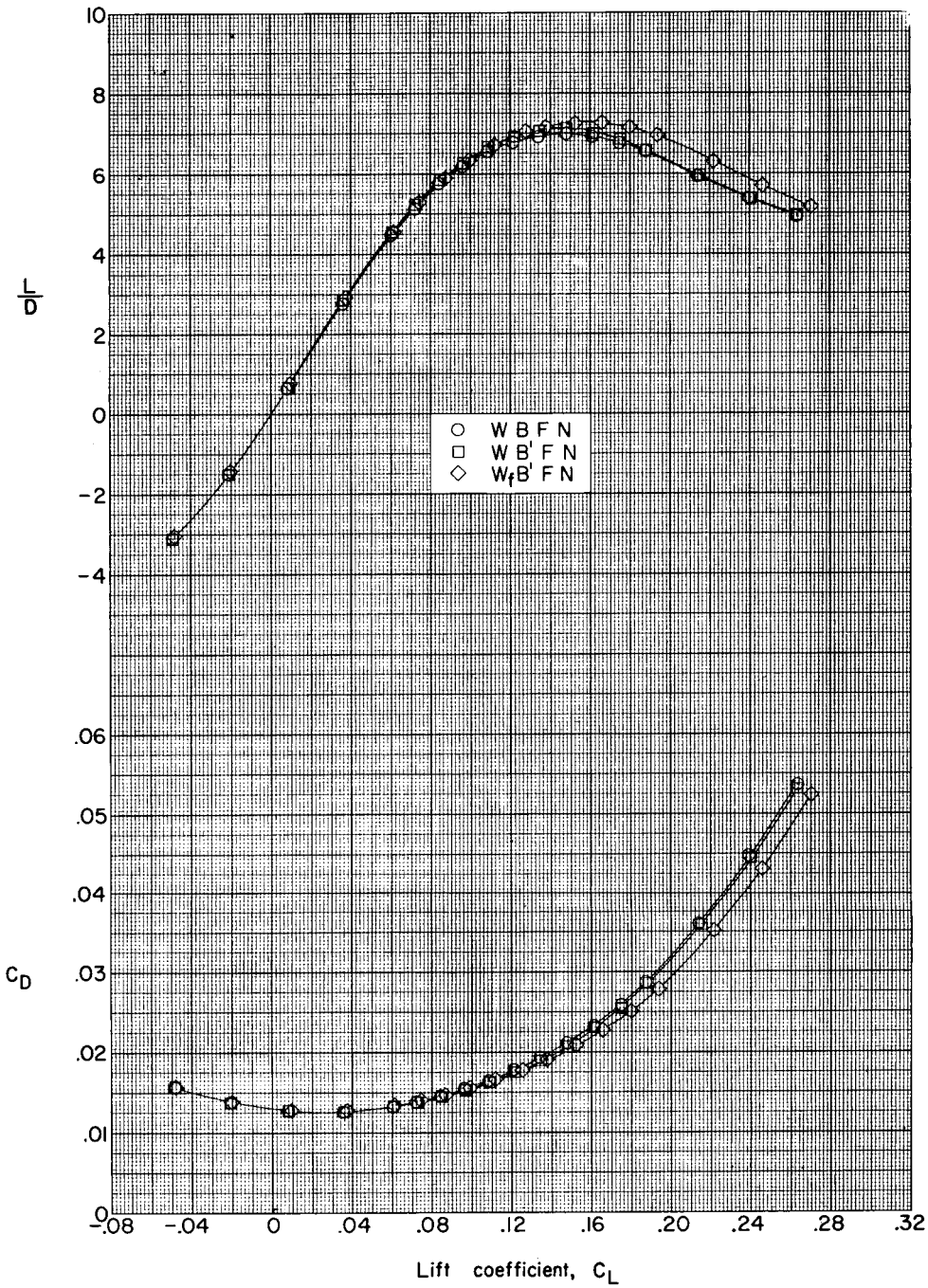

(b) Variation of L/D and C_D with C_L.

Figure 6.- Concluded.

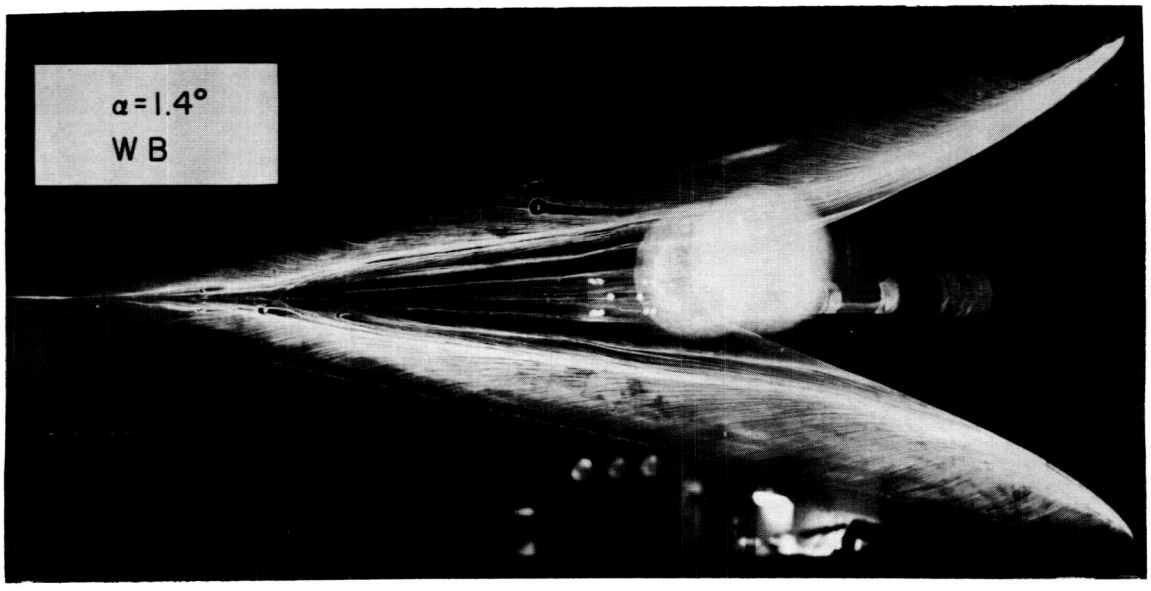

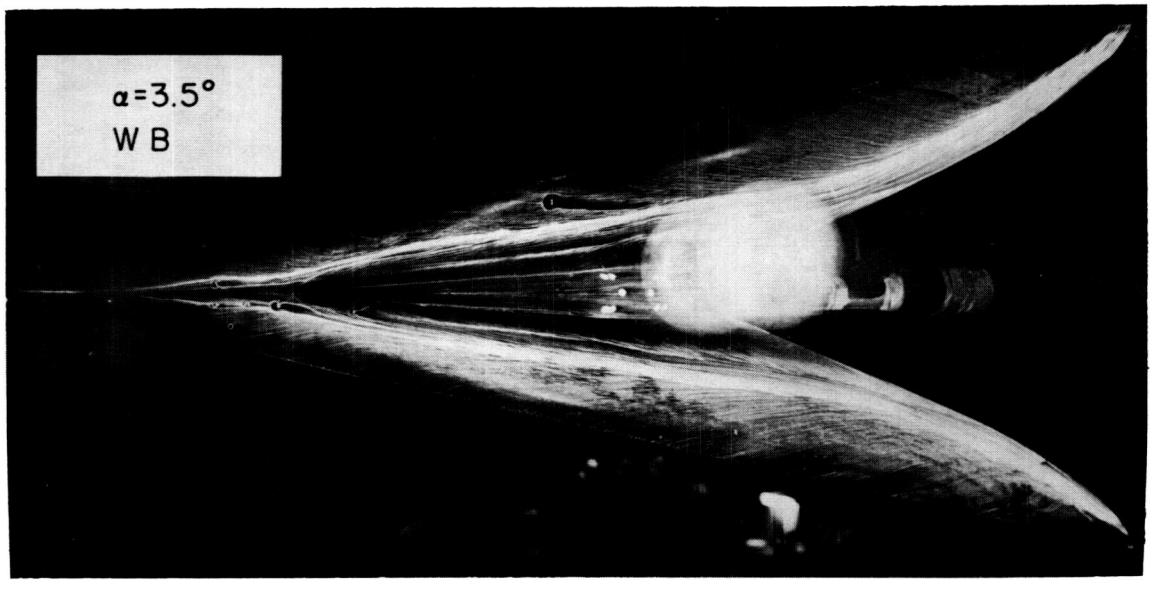

(a) Wing-body configuration. L-59-3017

Figure 7.- Luminescent-oil-flow photographs of configuration with original wing-apex section.

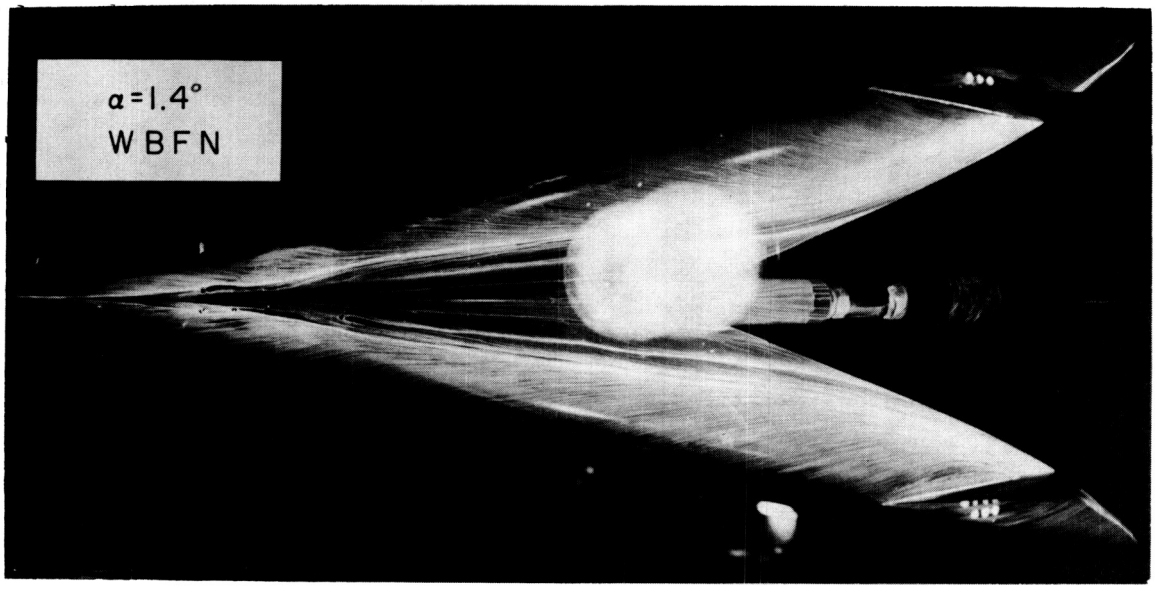

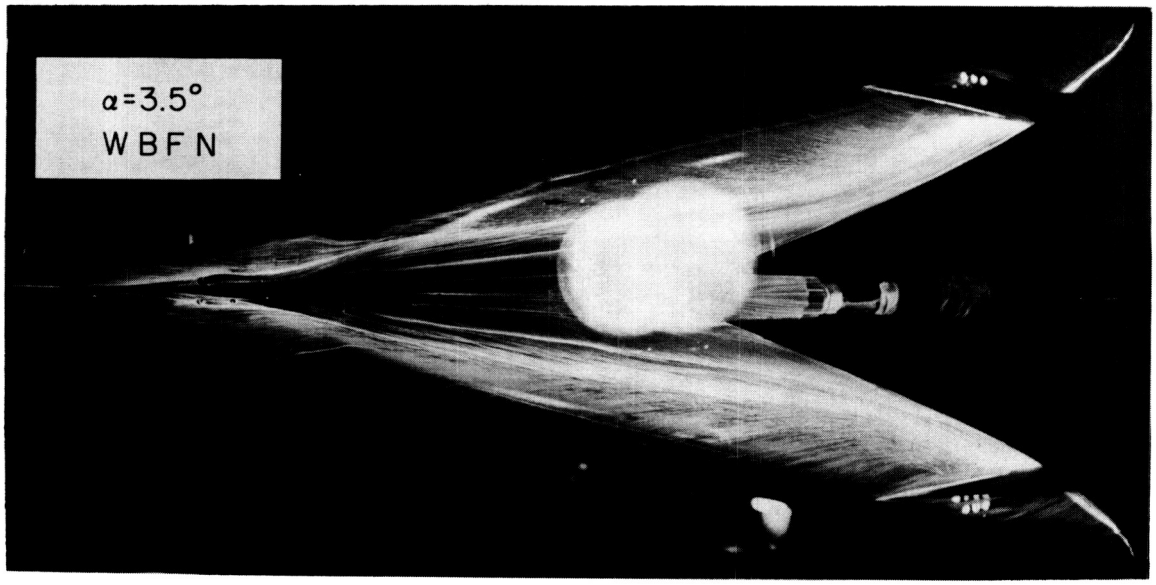

(b) Complete configuration. L-59-3018

Figure 7.- Concluded.

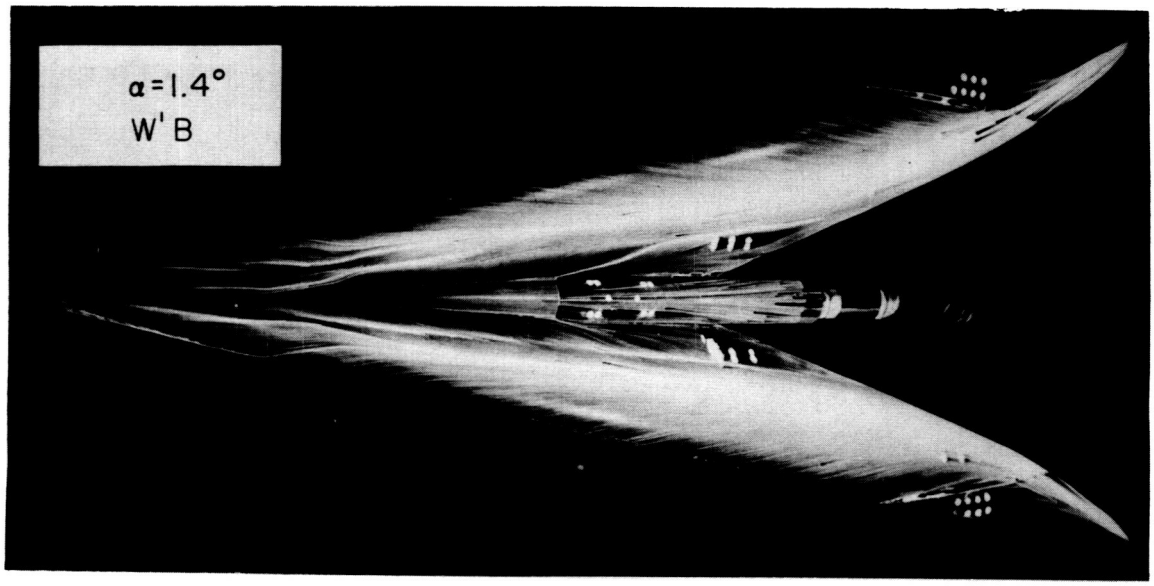

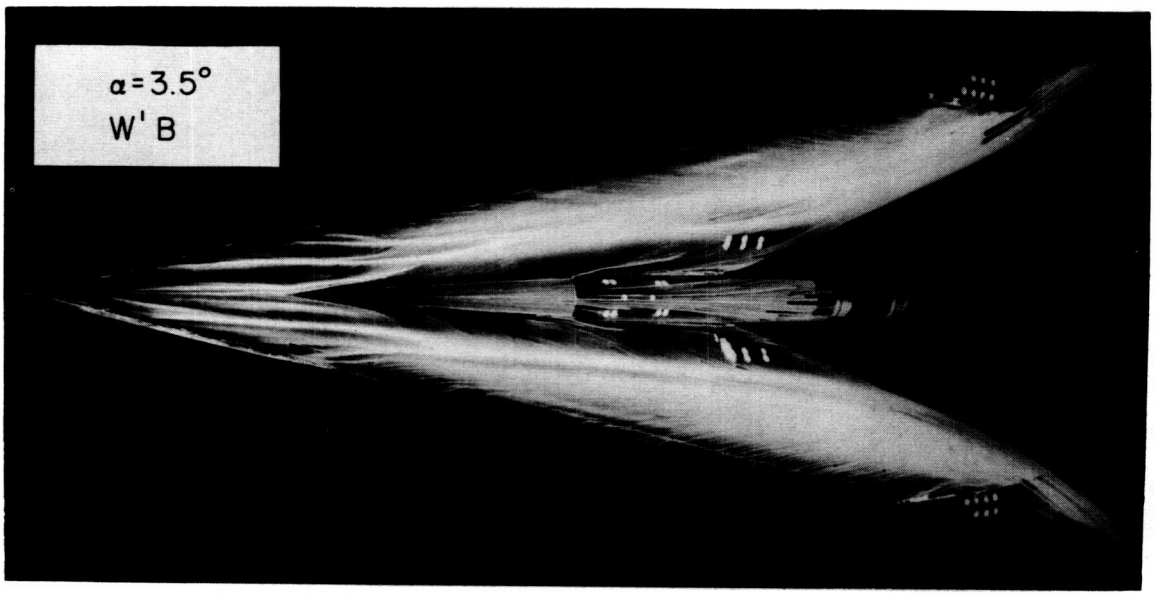

(a) Wing-body configuration. L-59-3019

Figure 8.- Luminescent-oil-flow photographs of configurations with modified wing-apex section.

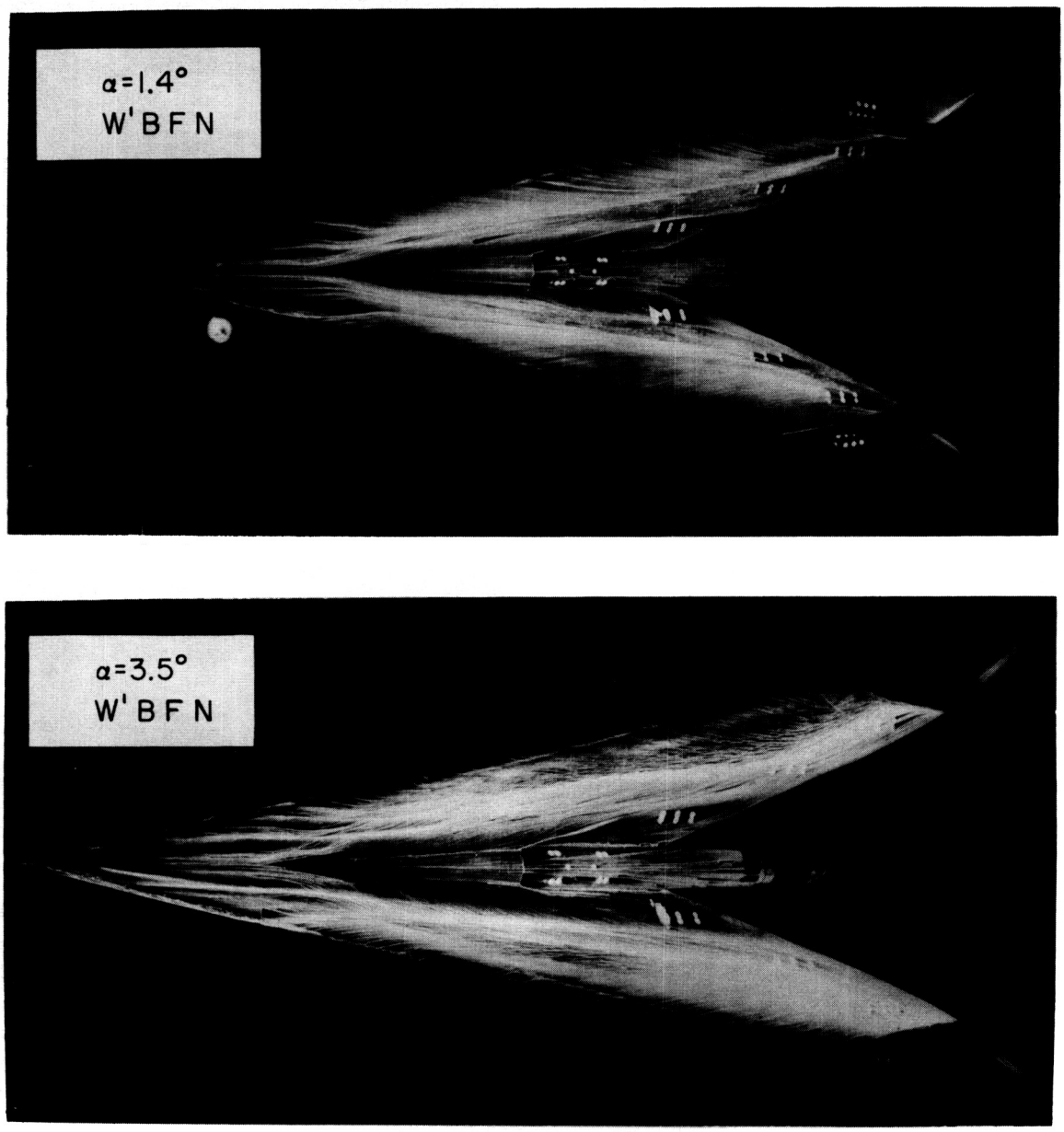

(b) Complete configuration. L-59-3020

Figure 8.- Concluded.

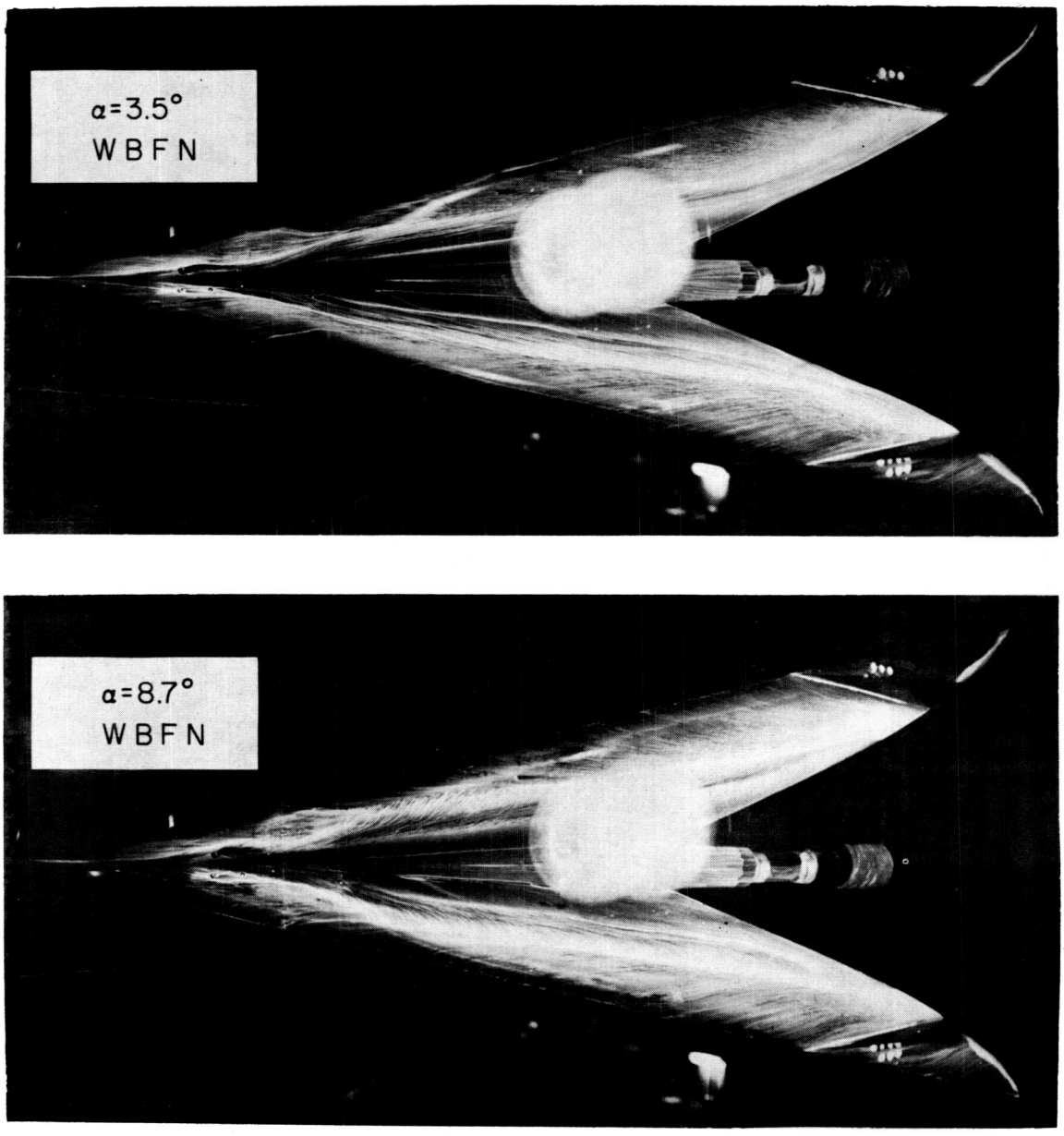

(a) Complete configuration. L-59-3021

Figure 9.- Luminescent-oil-flow photographs of complete model configuration with original wing-apex section.

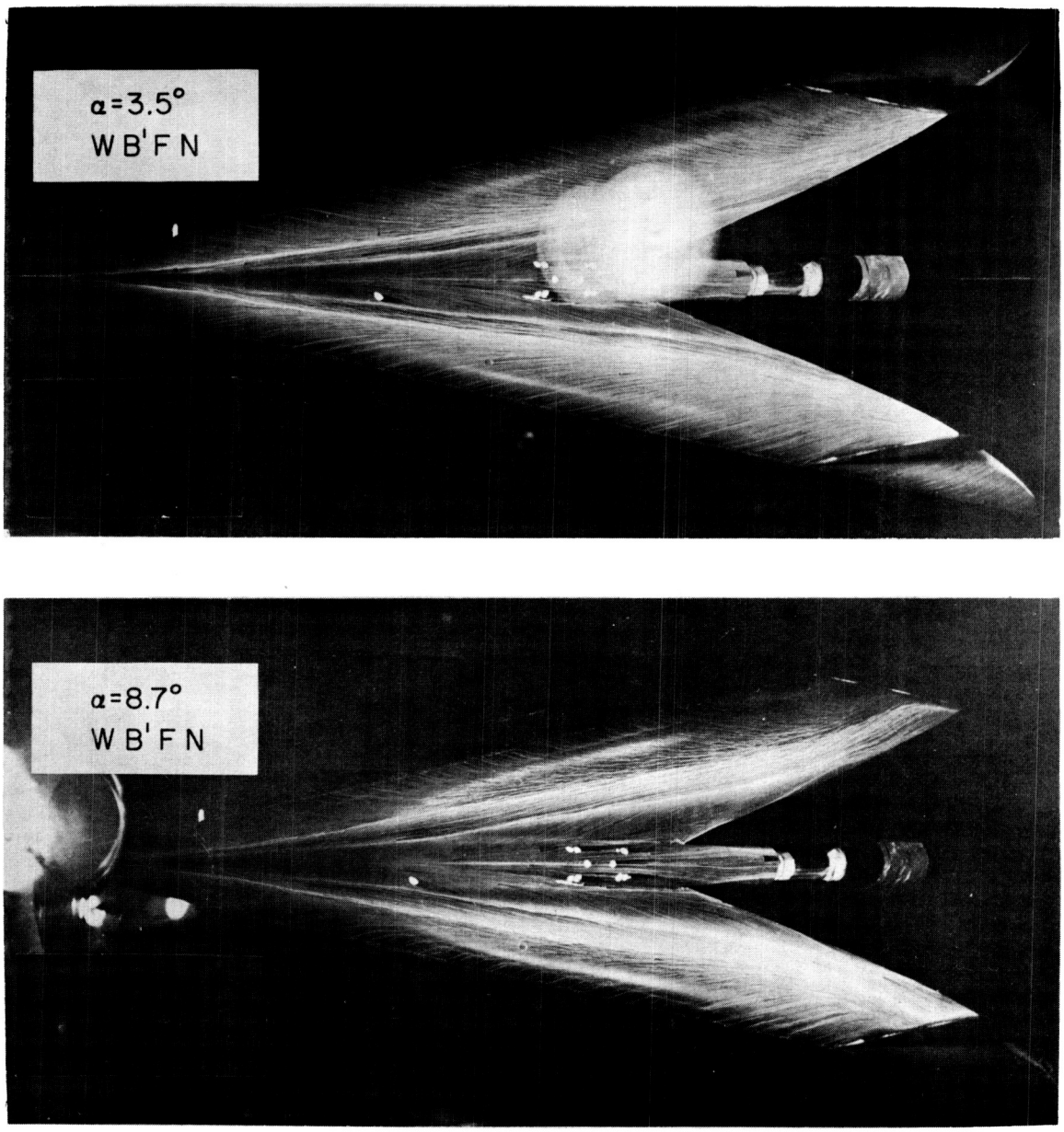

L-537

L-59-3022

(b) Complete configuration with wing-body juncture fairing.

Figure 9.- Concluded.

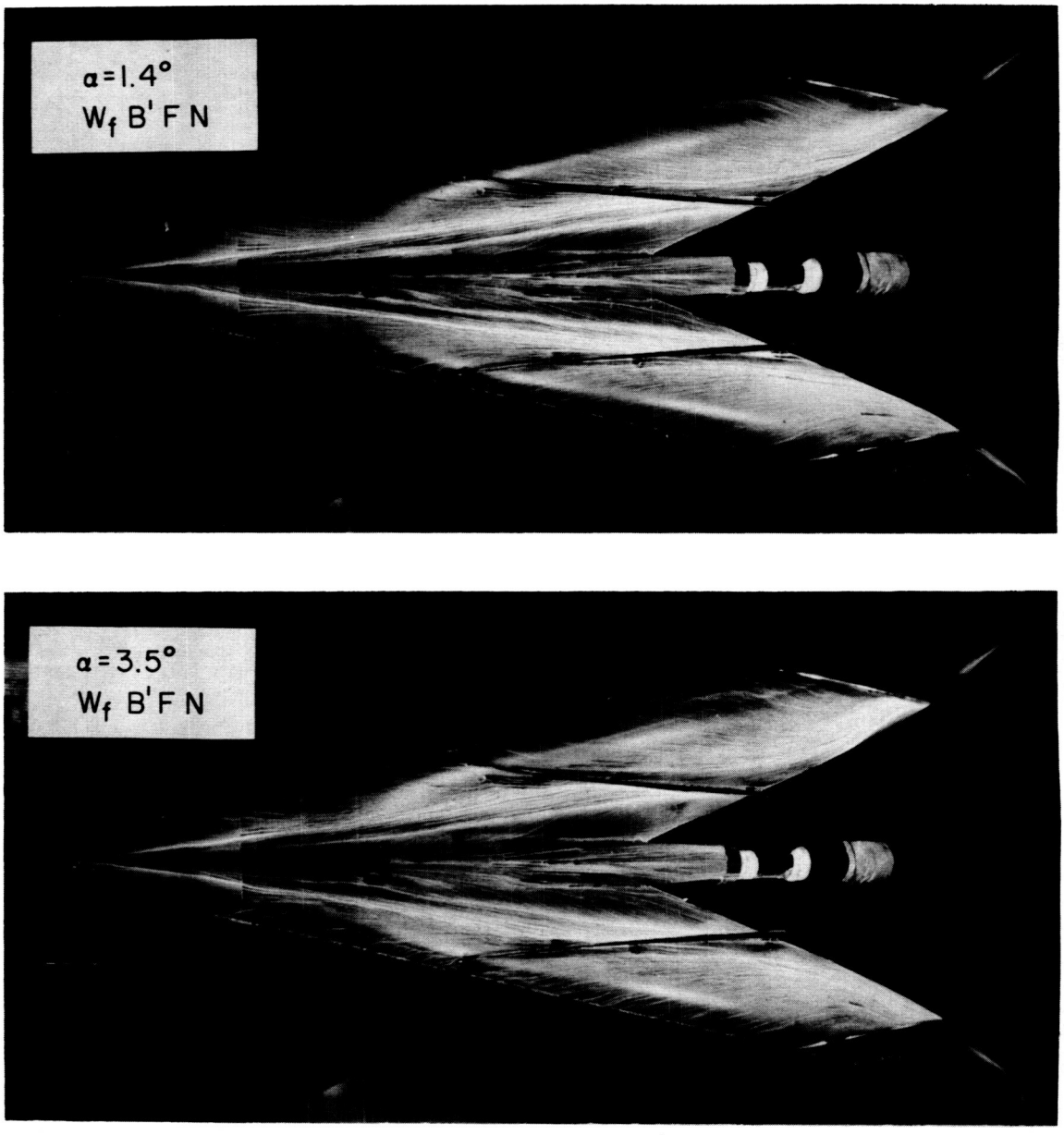

(a) $\alpha = 1.4^{\circ}$ and 3.5°. L-59-3023

Figure 10.- Complete configuration with original wing-apex section, wing-body-juncture fairings, and wing fences.

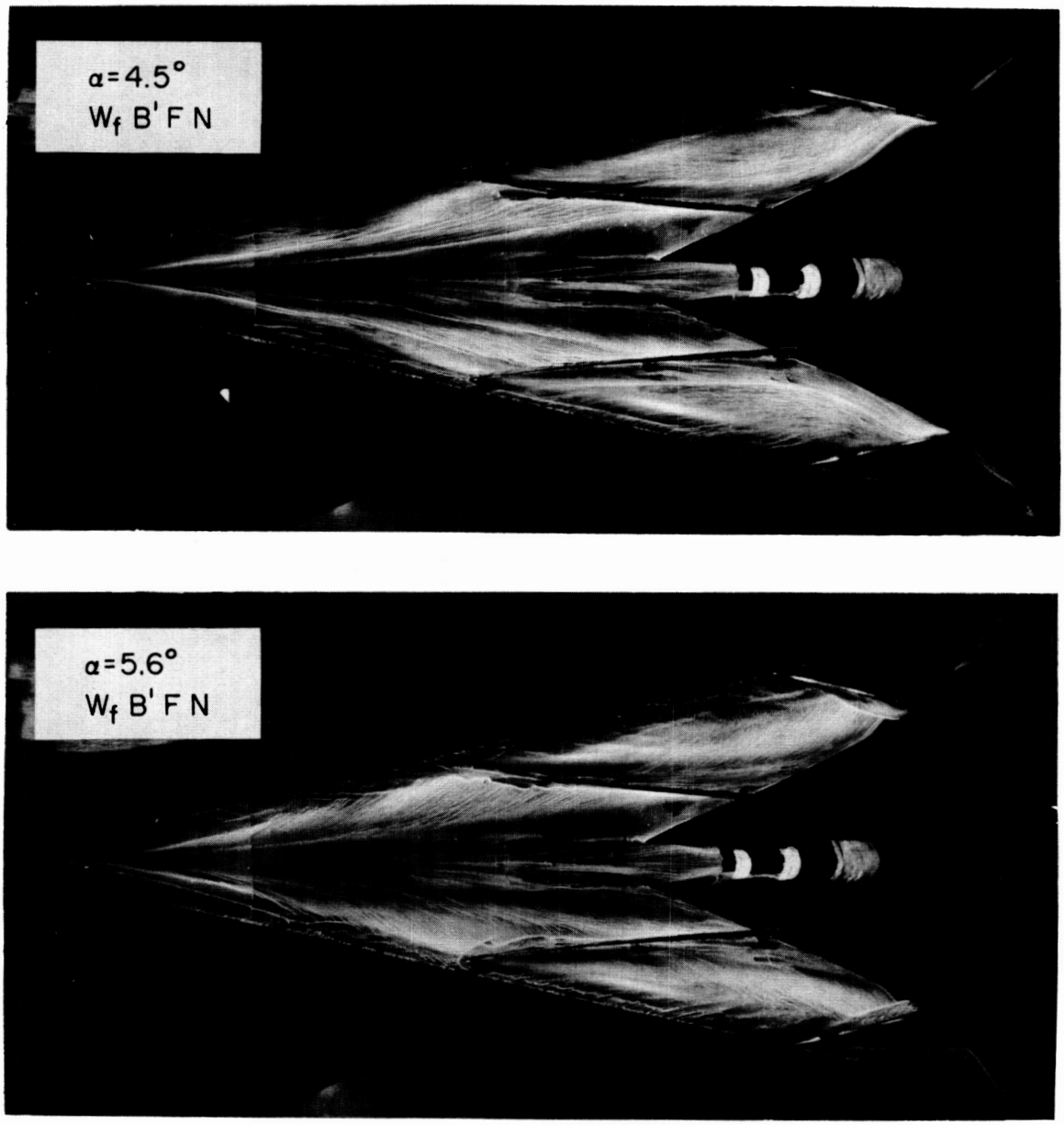

L-537

(b) $\alpha = 4.5^{\circ}$ and 5.6°. L-59-3024

Figure 10.- Concluded.

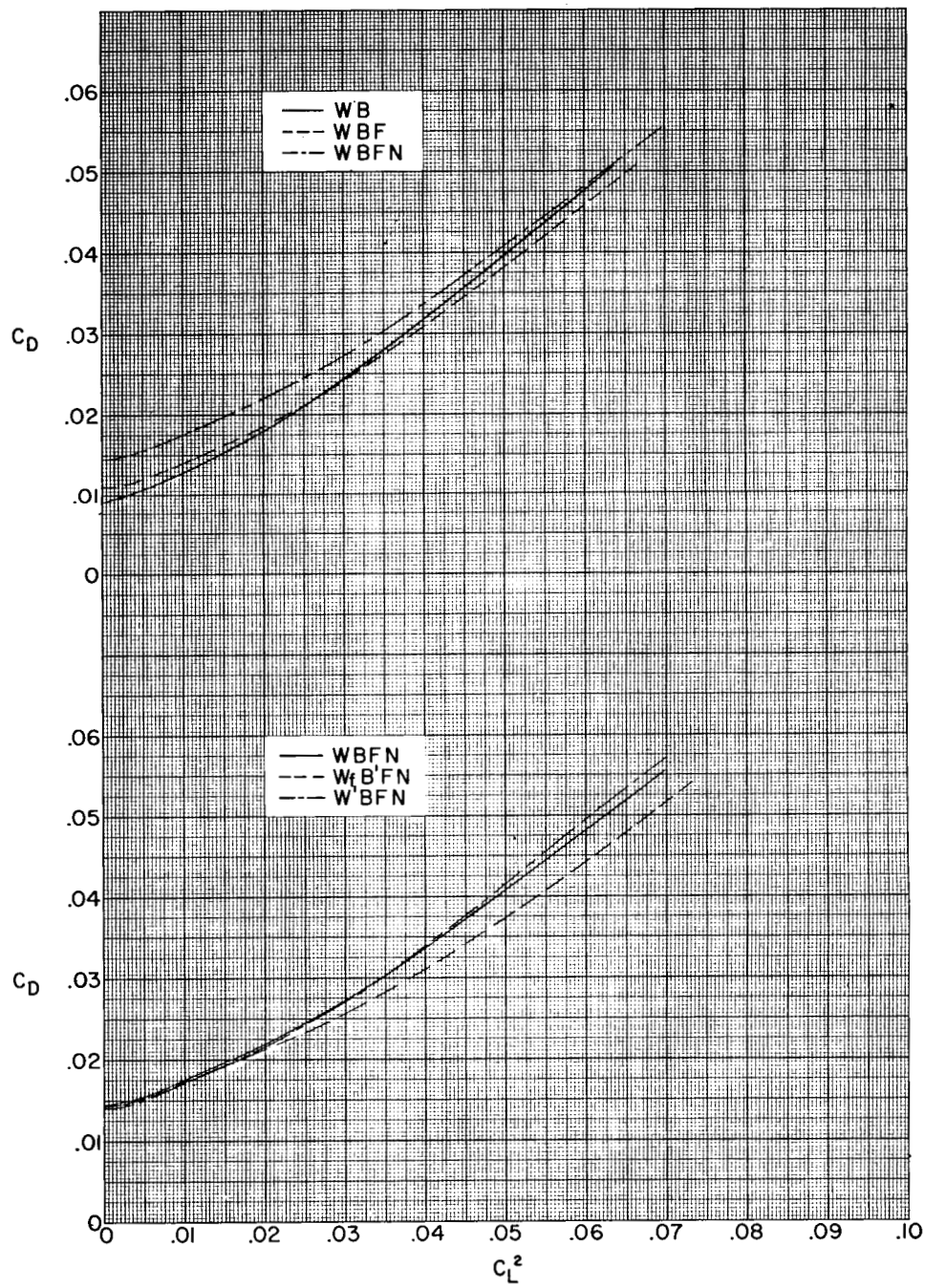

Figure 11.- Variation of C_D with C_L^2 for several model configurations.

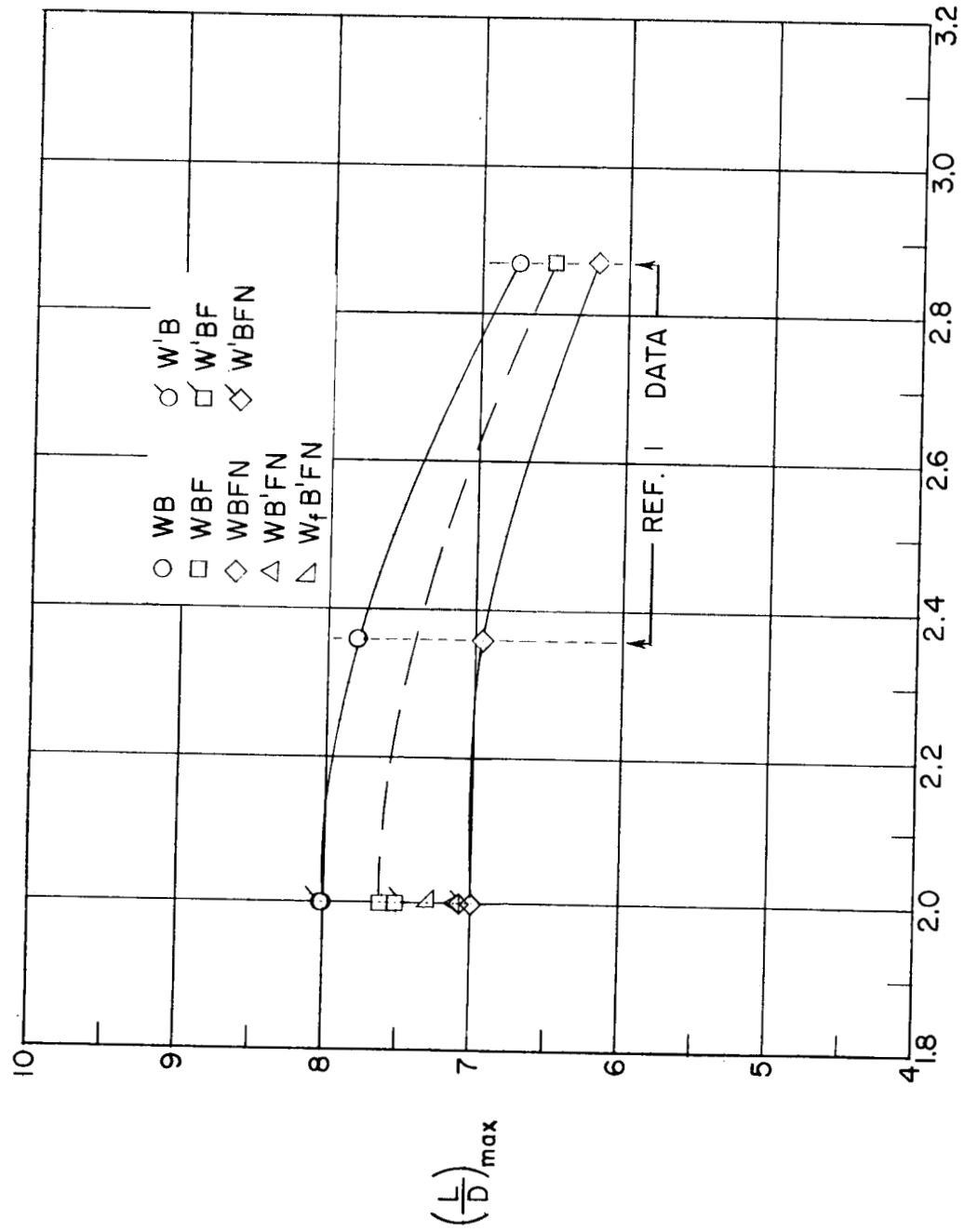

Figure 12.- Variation of maximum lift-drag ratio with Mach number for the various model configurations.